ACS APPLIED MATERIALS & INTERFACES

Research Article

www.acsami.org

Detoxification of a Sulfur Mustard Simulant Using a BODIPY-Functionalized Zirconium-Based Metal–Organic Framework

Ahmet Atilgan,[†] Timur Islamoglu,[†] Ashlee J. Howarth,[†] Joseph T. Hupp,[†] and Omar K. Farha*[,†,‡]

[†]Department of Chemistry, Northwestern University, 2145 Sheridan Road, Evanston, Illinois 60208, United States

[‡]Department of Chemistry, Faculty of Science, King Abdulaziz University, Jeddah 22254, Saudi Arabia

Supporting Information

ABSTRACT: Effective detoxification of chemical warfare agents is a global necessity. As a powerful photosensitizer, a halogenated BODIPY ligand is postsynthetically appended to the Zr_6 nodes of the metal–organic framework (MOF), NU-1000, to enhance singlet oxygen generation from the MOF. The BODIPY/MOF material is then used as a heterogeneous photocatalyst to produce singlet oxygen under green LED irradiation. The singlet oxygen selectively detoxifies the sulfur mustard simulant, 2-chloroethyl ethyl sulfide (CEES), to the less toxic sulfoxide derivative (2-chloroethyl ethyl sulfoxide, CEESO) with a half-life of approximately 2 min.

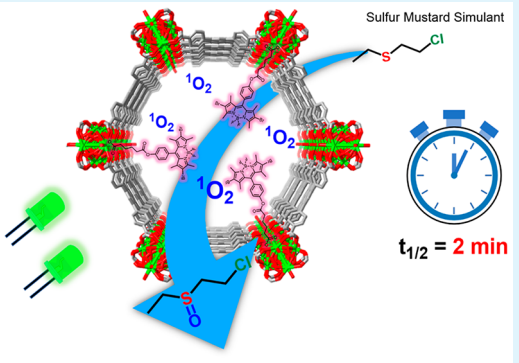

KEYWORDS: *BODIPY, mustard gas, sulfur mustard, CEES, singlet oxygen, photocatalyst, chemical warfare agents, metal–organic framework, heterogeneous catalysis*

INTRODUCTION

The degradation and removal of chemical warfare agents (CWAs) is a global challenge that has been present since chemical weapons were first used in combat.[1] Sulfur mustard, a strong blistering agent and vesicant that leads to severe eye, respiratory tract, and skin burns, is one of the most widely used CWAs due to its facile production.[2−4] Even though sulfur mustard and chemical weapons, in general, are prohibited by a global treaty signed in 1992 by 190 countries,[5] the use of sulfur mustard has been reported as recently as this year.[6,7] Thus, it is important to have efficient methods and materials for the detoxification of sulfur mustard in stockpiles and/or for protective clothing, masks, and other equipment. Sulfur mustard, bis(2-chloroethyl)sulfide, can be detoxified in three ways: hydrolysis, oxidation, and dehydrohalogenation (Scheme 1).

The hydrolysis and dehydrohalogenation pathways are generally too slow for practical use,[8,9] and therefore the oxidation pathway is our preferred method for detoxification. Overoxidation to the sulfone analogue, however, can pose problems for detoxification applications since the sulfone is also highly toxic.[10]

Bleaching powders have been previously studied for detoxification of sulfur mustard.[11] Some disadvantages of bleaching powders include the necessity of large amounts of powders (i.e., stoichiometric amounts or greater), corrosiveness, and decreasing effectiveness with extended storage. In addition to bleaching powder, metal oxides,[12−16] polyoxometalates,[17,18] and polymer networks[19] have been studied.

Scheme 1. Detoxification Pathways of Sulfur Mustard

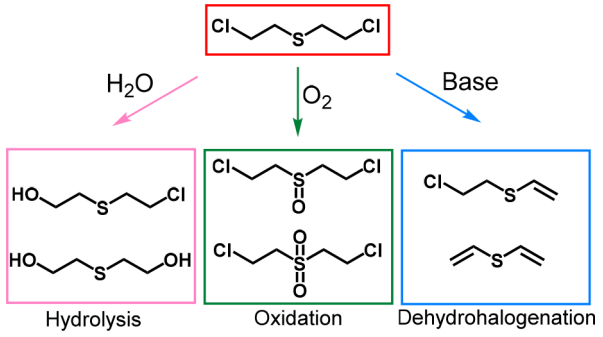

However, none of these are yet fully satisfactory for fast, selective, safe, and efficient oxidative detoxification of sulfur mustard.

Selective oxidation of sulfur mustard can be accomplished using singlet oxygen which can be produced from ground-state O_2 (triplet oxygen) using a photosensitizer.[20] Among organic-based photosensitizers, BODIPY (boron-dipyrromethene) derivatives have drawn significant attention due to their wide-ranging chemical and photophysical properties.[21] For example, BODIPY can be easily modified by the addition of heavy halogen atoms such as iodine or bromine, which have been

Received: April 19, 2017
Accepted: June 27, 2017
Published: June 27, 2017

DOI: 10.1021/acsami.7b05494
ACS Appl. Mater. Interfaces 2017, 9, 24555−24560

shown to enhance the efficiency of BODIPY as a singlet oxygen photosensitizer.[22,23] As a consequence of its highly modular and tunable nature, BODIPY has been explored for many applications including photodynamic therapy,[24−26] molecular sensing,[27] and catalysis.[28,29]

Metal−organic frameworks (MOFs) are porous crystalline materials comprised of metal nodes and organic linkers.[30−35] MOFs have gained tremendous attention due to their structural tunability and can be tailored to have ultrahigh porosity and chemical and thermal stability.[36−39] Therefore, MOFs have been studied for numerous potential applications such as catalysis,[40,41] gas storage and separation,[42−45] and chemical sensing.[46,47] Among the various applications, the use of MOFs as catalysts[48−53] or catalyst supports[54−56] has drawn great attention, in part due to their atomically well-defined structures. We have previously shown that Zr-based MOFs are promising candidates for photosensitizer incorporation and subsequently for the catalytic and selective oxidation of sulfur mustard using singlet oxygen. Using different organic struts comprising porphyrin[57] or pyrene[58] moieties, selective (photosensitized) oxidation of the sulfur mustard simulant 2-chloroethyl ethyl sulfide (CEES) to 2-chloroethyl ethyl sulfoxide (CEESO) was observed with half-lives of 13 or 6 min, respectively. While the structural organic linkers of MOFs can be employed as photosensitizers, nonstructural ligands can also be incorporated in Zr-MOFs, most notably by solvent-assisted ligand incorporation (SALI).[59,60] SALI is a postsynthetic modification method whereby terminal aqua and hydroxo groups on the Zr_6 node are displaced by carboxylate[59,61−67] (or phosphonate)[64,68] groups. We have recently reported the incorporation of a fullerene-based photosensitizer for singlet oxygen into a Zr-based MOF via SALI, and the resulting material showed a remarkable half-life for CEES oxidation of 3.5 min.[69] However, fullerenes are synthetically challenging to produce[70] and modify due to their low solubility.[71] In addition, fullerenes demonstrate poor optical and electronic tunability[72] and low absorption efficiency across the visible spectrum,[70] which limits the ability to study fullerenes further for this application. It is therefore necessary to seek new materials for the detoxification of CEES (and hence sulfur mustard) that are even faster. Hereby, we demonstrate fast and selective detoxification of a mustard gas simulant (CEES) using NU-1000 modified with a highly tunable BODIPY chromophore (Figure 1).

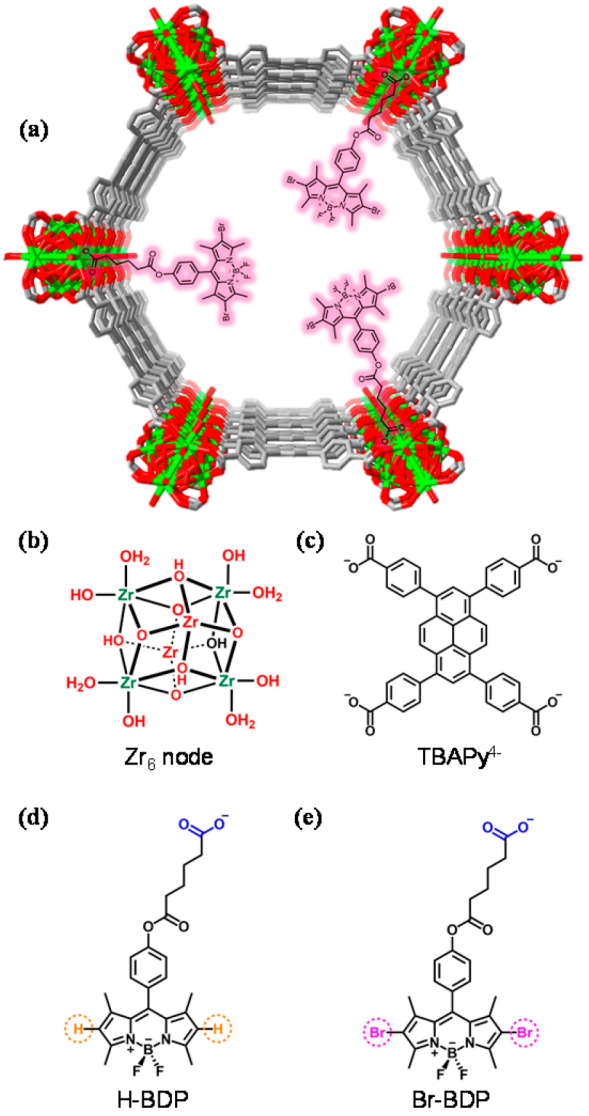

Figure 1. (a) Schematic representation of Br-BDP@NU-1000; (b) Zr_6 node of NU-1000, with SALI-displaceable aqua and hydroxy ligands shown in green; (c) structure of organic linker of NU-1000, (d) H-BDP, and (e) Br-BDP.

EXPERIMENTAL SECTION

The BODIPY photosensitizers (H-BDP and Br-BDP, Figure 1(d) and (e), respectively) were synthesized as described in the Supporting Information. Br-BDP was incorporated into NU-1000 via SALI by taking Br-BDP (86 mg, 0.15 mmol) dissolved in 4 mL of acetonitrile and adding NU-1000 (30 mg, 0.015 mmol). The mixture was then stirred at 300 rpm with a magnetic stirrer at 60 °C for 24 h. The solid was separated by centrifugation and washed several times with fresh and warm acetonitrile followed by Soxhlet extraction with dichloromethane and methanol (see Supporting Information). The BODIPY loading was determined to be about 0.75/Zr_6 node using X-ray fluorescence (XRF) spectroscopy.

To test the photocatalytic activity of each material, the photosensitizer (PS) or PS-loaded MOF was dissolved or dispersed in 1 mL of anhydrous methanol in a 17 × 83 mm glass microwave vial with a magnetic stir bar. The microwave vial was then sealed tightly, and the mixture was purged with O_2 for 20 min. An amount of 10 μL (0.08 mmol) of internal standard (1-bromo-3,5-difluorobenzene) and 23 μL (0.2 mmol) of 2-chloroethyl ethyl sulfide (CEES) were injected into the vial using a microsyringe. Aliquots were taken from the reaction vial using a syringe at different time intervals and diluted to 0.8 mL with dichloromethane. Samples were then introduced to a GC-FID instrument to monitor the reaction kinetics. Both progress and selectivity of the oxidation were screened at various times using ^{1}H and ^{13}C NMR spectroscopy (Figures S4−S5). Two commercially available green LEDs (ems@520−535 nm, 450 mW power) and two cyan LEDs (ems@490−520 nm, 200 mW power) were used to excite Br-BDP (abs@525 nm) and H-BDP (abs@499 nm), respectively. (See Supporting Information for details of the irradiation assembly.)

RESULTS AND DISCUSSION

As depicted in Figure 1, we installed a carboxylic acid terminated chain on the meso position of the BODIPY chromophore which allows for the incorporation of BODIPY in NU-1000 by tethering the ligand to the Zr_6 node. BODIPY was chosen as a chromophore for singlet oxygen generation due to its facile synthesis, ease of tunability, and high solubility in numerous organic solvents, including solvents suitable for SALI. It is well-documented that functionalizing BODIPY with heavy atoms (e.g., bromine or iodine) increases its efficiency as a photosensitizer for singlet oxygen due to enhanced

DOI: 10.1021/acsami.7b05494
ACS Appl. Mater. Interfaces 2017, 9, 24555−24560

intersystem crossing, i.e., photoexcited BODIPY singlet to excited triplet state conversion.[22,23] Therefore, we synthesized carboxylic acid functionalized Br-BDP (Figure 1e) and compared it to Br-BDP after installation in NU-1000. The loading of Br-BDP was measured to be about 0.75 Br-BDP/Zr_6 node.

Figure 2 shows the oxidation of CEES using BODIPY as a photosensitizer for singlet oxygen in both homogeneous and heterogeneous forms. As anticipated for a process limited by singlet oxygen availability, Br-BDP engendered much faster conversion (oxidation) compared to H-BDP under homogeneous reaction conditions (approximate half-lives: 2.5 vs 19.5 min, respectively, at power density of irradiation = 200 mW cm^{-2}) (Figure 2a). As a result, Br-BDP was incorporated into NU-1000 to test its ability as a heterogeneous photosensitizer.

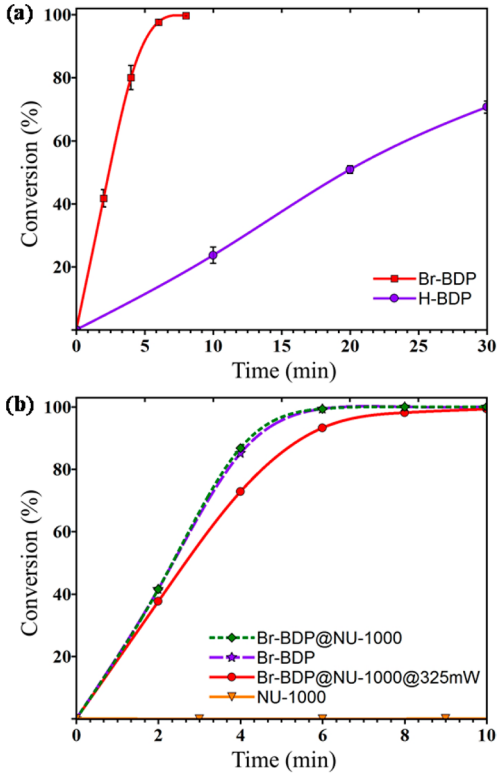

Figure 2. (a) Oxidation of CEES over time with Br-BDP and H-BDP catalysts in a homogeneous phase under 200 mW cm^{-2} green and cyan LED light, respectively. (b) Comparison of oxidation of CEES with Br-BDP in the homo/heterogeneous phase and NU-1000 under 450 mW cm^{-2} green light. Comparison of catalytic efficiency of Br-BDP@NU-1000 under 325 mW and 450 mW light power.

In Figure 2b, the efficacy of Br-BDP is compared for the heterogeneous (MOF) versus homogeneous phase. Half-lives for CEES oxidation were observed to be approximately 2 min in each case (power density of irradiation = 450 mW cm^{-2}). The power of the LEDs used was then decreased using a dimmable driver to 325 mW cm^{-2} to compare the BODIPY system with our previous studies where blue LEDs were used at 325 mW cm^{-2} to excite a porphyrin chromophore.[57] The conversion profile is shown in Figure 2b, demonstrating that the photooxidation reaction of CEES under the diminished light intensity results in a half-life of approximately 2.5 min. It is worth noting that NU-1000 alone displays negligible catalytic activity under green LED irradiation, consistent with its transparency in the green part of the spectrum. These findings establish that Br-BDP is solely responsible for the singlet oxygen production from Br-BDP@NU-1000. Importantly, oxidation of CEES using Br-BDP as a photocatalyst for singlet oxygen generation only yields the less toxic sulfoxide product, CEESO, as evidenced by ^{1}H and ^{13}C NMR spectroscopy (Figures S4–S5).

For comparison, shown in Table 1 are half-lives and light intensities for photo-oxidation of CEES with catalytically sensitized Br-BDP@NU-1000 versus other MOF-based sensitizers. As estimated by reaction half-lives, photo-oxidation based on Br-BDP@NU-1000 sensitization is nearly twice as fast as the fastest of the three previously investigated systems. When compared to a porphyrin-based MOF catalyst run under 325 mW cm^{-2} blue LED irradiation, the Br-BDP@NU-1000-sensitized oxidation has about 5 times faster half-life under equal irradiation power. Notably, even very low photocatalyst loadings (0.2 mol % Br-BDP@NU-1000) proved effective for CEES degradation by dioxygen.

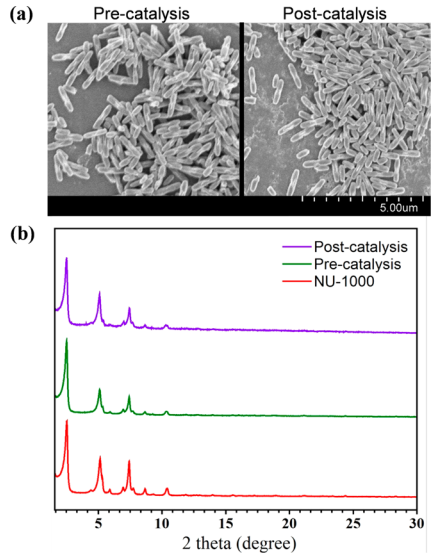

Figure 3. (a) SEM images of Br-BDP@NU-1000 crystals before and after photooxidation and (b) powder X-ray diffraction patterns of NU-1000, Br-BDP@NU-1000, and Br-BDP@NU-1000 after catalysis.

Table 1. Comparison of the Half-Lives for CEES Oxidation Using MOF-Based Photosensitizers for Singlet Oxygen Production

catalyst	catalyst/CEES ratio	solvent	photosensitizer	LED type and power (mW cm^{-2})	half-life (min)	reference
PCN-222	1%	MeOH	porphyrin	blue (325)	13	57
NU-1000	1%	MeOH	pyrene	UV (450)	~6	58
NU-1000-PCBA	1%	MeOH	pyrene-fullerene	UV (450)	3.5	69
Br-BDP@NU-1000	0.2%	MeOH	BODIPY	green (325)	~2.5	this study
Br-BDP@NU-1000	0.2%	MeOH	BODIPY	green (450)	~2	this study

DOI: 10.1021/acsami.7b05494
ACS Appl. Mater. Interfaces 2017, 9, 24555–24560

The structural integrity of Br-BDP@NU-1000 before and after catalysis was confirmed using powder X-ray diffraction (PXRD), while scanning electron microscopy (SEM) revealed that the morphology of the crystals was unchanged (Figure 3). An SEM-EDX line scan analysis performed on a crystal of Br-BDP@NU-1000 shows an unvarying ratio of Br to Zr, implying that Br-BDP is homogeneously distributed in the MOF. Furthermore, the recyclability of Br-BDP@NU-1000 was tested over four cycles, irradiating for 9 min each time (Figure S7). Full conversion of CEES to the less toxic CEESO was observed for the first three cycles, while conversion decreased to 80% in the fourth 9 min cycle, likely due to photobleaching of the catalyst.

CONCLUSION

In conclusion, we have observed facile incorporation (via SALI) of a very efficient and, in principle, chemically tunable photosensitizer, Br-BDP, into a stable Zr-based MOF. Photoexcitation catalyzes the conversion of ground-state (triplet) oxygen to reactive singlet oxygen and, in turn, the fast and selective oxidation of the sulfur mustard simulant, CEES, to the less toxic sulfoxide product, CEESO. Notably, the Br-BDP-functionalized MOF retains crystallinity under catalysis conditions. Importantly, the photooxidation method makes use of readily available and inexpensive LEDs, synthetically tunable BODIPY molecules, and a simple incorporation method (SALI) which should enable screening of a wide range of BODIPY and related chromophores as photosensitizers for sulfur-mustard detoxification.

ASSOCIATED CONTENT

Supporting Information

The Supporting Information is available free of charge on the ACS Publications website at DOI: 10.1021/acsami.7b05494.

General experimental; synthesis of compounds; solvent-assisted ligand incorporation (SALI) procedure; oxidation of CEES (sulfur mustard simulant); nitrogen isotherms and pore-size distribution; drifts spectra; singlet oxygen generation test; recyclability test; selectivity tests; absorption spectra; emission spectra of LEDs; X-ray fluorescence (XRF) results; NMR spectra; mass spectra; references (PDF)

AUTHOR INFORMATION

Corresponding Author

*O. K. Farha. E-mail: o-farha@northwestern.edu.

ORCID

Ahmet Atilgan: 0000-0002-1531-3996
Timur Islamoglu: 0000-0003-3688-9158
Joseph T. Hupp: 0000-0003-3982-9812
Omar K. Farha: 0000-0002-9904-9845

Notes

The authors declare no competing financial interest.

ACKNOWLEDGMENTS

The authors gratefully acknowledge support from the Army Research Office (project no. W911NF-13-1-0229). A.J.H. thanks NSERC for a postdoctoral fellowship.

REFERENCES

(1) Ghabili, K.; Agutter, P. S.; Ghanei, M.; Ansarin, K.; Panahi, Y.; Shoja, M. M. Sulfur Mustard Toxicity: History, Chemistry, Pharmacokinetics, and Pharmacodynamics. *Crit. Rev. Toxicol.* **2011**, *41*, 384−403.

(2) Geraci, M. J. Mustard Gas: Imminent Danger or Eminent Thread. *Ann. Pharmacother.* **2008**, *42*, 237−246.

(3) Szinicz, L. History of Chemical and Biological Warfare Agents. *Toxicology* **2005**, *214*, 167−181.

(4) Fitzgerald, G. J. Chemical Warfare and Medical Response During World War I. *Am. J. Public Health* **2008**, *98*, 611−625.

(5) Organisation for the Prohibition of Chemical Weapons. Chemical Weapons Convention. https://www.opcw.org/chemical-weapons-convention/ (accessed on January 22, 2017).

(6) Khadder, K.; Elwazer, S.; Roberts, E.; Kourdi, E.; Qiblawi, T. Suspected Gas Attack in Syria Reportedly Kills Dozens. http://www.cnn.com/2017/04/04/middleeast/idlib-syria-attack/index.html (accessed on March 04, 2017).

(7) Fassihi, F. U. N. Report Finds Chemical Weapons Used by Syrian Regime, Islamic State. *The Wall Street Journal* [Online], 2016. https://www.wsj.com/articles/u-n-report-finds-chemical-weapons-used-by-syrian-regime-islamic-state-1472092954 (accessed on January 22, 2017).

(8) Herriott, R. M. Solubility of Mustard Gas [Bis (ß-Chloroethyl) Sulfide] in Water, Molar Sodium Chloride, and in Solutions of Detergents. *J. Gen. Physiol.* **1947**, *30*, 449−456.

(9) Smith, B. M. Catalytic Methods for the Destruction of Chemical Warfare Agents under Ambient Conditions. *Chem. Soc. Rev.* **2007**, *37*, 470−478.

(10) Hirade, J.; Ninomiya, A. Studies on the Mechanism of the Toxic Action of Organic Halogen Compounds. *J. Biochem.* **1950**, *37*, 19−34.

(11) Kim, K.; Tsay, O. G.; Atwood, D. A.; Churchill, D. G. Destruction and Detection of Chemical Warfare Agents. *Chem. Rev.* **2011**, *111*, 5345−5403.

(12) Wagner, G. W.; Bartram, P. W.; Koper, O.; Klabunde, K. J. Reactions of VX, GD, and HD with Nanosize Mgo. *J. Phys. Chem. B* **1999**, *103*, 3225−3228.

(13) Wagner, G. W.; Koper, O. B.; Lucas, E.; Decker, S.; Klabunde, K. J. Reactions of VX, GD, and HD with Nanosize Cao: Autocatalytic Dehydrohalogenation of HD. *J. Phys. Chem. B* **2000**, *104*, 5118−5123.

(14) Panayotov, D. A.; Paul, D. K.; Yates, J. T. Photocatalytic Oxidation of 2-Chloroethyl Ethyl Sulfide on Tio2−Sio2 Powders. *J. Phys. Chem. B* **2003**, *107*, 10571−10575.

(15) Ramacharyulu, P. V. R. K.; Kumar, J. P.; Prasad, G. K.; Singh, B.; Sreedhar, B.; Dwivedi, K. Sunlight Assisted Photocatalytic Detoxification of Sulfur Mustard on Vanadium Ion Doped Titania Nanocatalysts. *J. Mol. Catal. A: Chem.* **2014**, *387*, 38−44.

(16) Wagner, G. W.; Procell, L. R.; Yang, Y.-C.; Bunton, C. A. Molybdate/Peroxide Oxidation of Mustard in Microemulsions. *Langmuir* **2001**, *17*, 4809−4811.

(17) Gall, R. D.; Faraj, M.; Hill, C. L. Role of Water in Polyoxometalate-Catalyzed Oxidations in Nonaqueous Media. Scope, Kinetics, and Mechanism of Oxidation of Thioether Mustard (HD) Analogs by Tert-Butyl Hydroperoxide Catalyzed by H5PV2Mo10O40. *Inorg. Chem.* **1994**, *33*, 5015−5021.

(18) Gall, R. D.; Hill, C. L.; Walker, J. E. Carbon Powder and Fiber-Supported Polyoxometalate Catalytic Materials. Preparation, Characterization, and Catalytic Oxidation of Dialkyl Sulfides as Mustard (HD) Analogues. *Chem. Mater.* **1996**, *8*, 2523−2527.

(19) Bromberg, L.; Pomerantz, N.; Schreuder-Gibson, H.; Hatton, T. A. Degradation of Chemical Threats by Brominated Polymer Networks. *Ind. Eng. Chem. Res.* **2014**, *53*, 18761−18774.

(20) Ghogare, A. A.; Greer, A. Using Singlet Oxygen to Synthesize Natural Products and Drugs. *Chem. Rev.* **2016**, *116*, 9994−10034.

(21) Loudet, A.; Burgess, K. BODIPY Dyes and Their Derivatives: Synthesis and Spectroscopic Properties. *Chem. Rev.* **2007**, *107*, 4891−4932.

DOI: 10.1021/acsami.7b05494
ACS Appl. Mater. Interfaces 2017, 9, 24555−24560

(22) Zhang, X. F.; Yang, X. Singlet Oxygen Generation and Triplet Excited-State Spectra of Brominated BODIPY. *J. Phys. Chem. B* **2013**, *117*, 5533−5539.
(23) Yogo, T.; Urano, Y.; Ishitsuka, Y.; Maniwa, F.; Nagano, T. Highly Efficient and Photostable Photosensitizer Based on BODIPY Chromophore. *J. Am. Chem. Soc.* **2005**, *127*, 12162−12163.
(24) Kamkaew, A.; Lim, S. H.; Lee, H. B.; Kiew, L. V.; Chung, L. Y.; Burgess, K. BODIPY Dyes in Photodynamic Therapy. *Chem. Soc. Rev.* **2013**, *42*, 77−88.
(25) Atilgan, A.; Eçik, E. T.; Guliyev, R.; Uyar, T. B.; Erbas-Cakmak, S.; Akkaya, E. U. Near-Ir-Triggered, Remote-Controlled Release of Metal Ions: A Novel Strategy for Caged Ions. *Angew. Chem., Int. Ed.* **2014**, *53*, 10678−10681.
(26) Ecik, E. T.; Atilgan, A.; Guliyev, R.; Uyar, T. B.; Gumus, A.; Akkaya, E. U. Modular Logic Gates: Cascading Independent Logic Gates Via Metal Ion Signals. *Dalton Trans.* **2014**, *43*, 67−70.
(27) Yang, S. K.; Shi, X.; Park, S.; Ha, T.; Zimmerman, S. C. A Dendritic Single-Molecule Fluorescent Probe That Is Monovalent, Photostable and Minimally Blinking. *Nat. Chem.* **2013**, *5*, 692−697.
(28) Luo, G.-G.; Fang, K.; Wu, J.-H.; Dai, J.-C.; Zhao, Q.-H. Noble-Metal-Free BODIPY-Cobaloxime Photocatalysts for Visible-Light-Driven Hydrogen Production. *Phys. Chem. Chem. Phys.* **2014**, *16*, 23884−23894.
(29) Quan, Y.; Li, Q.-Y.; Zhang, Q.; Zhang, W.-Q.; Lu, H.; Yu, J.-H.; Chen, J.; Zhao, X.; Wang, X.-J. A Diiodo-BODIPY Postmodified Metal-Organic Framework for Efficient Heterogeneous Organo-Photocatalysis. *RSC Adv.* **2016**, *6*, 23995−23999.
(30) Férey, G.; Mellot-Draznieks, C.; Serre, C.; Millange, F.; Dutour, J.; Surblé, S.; Margiolaki, I. A Chromium Terephthalate-Based Solid with Unusually Large Pore Volumes and Surface Area. *Science* **2005**, *309*, 2040−2042.
(31) Furukawa, H.; Cordova, K. E.; O'Keeffe, M.; Yaghi, O. M. The Chemistry and Applications of Metal-Organic Frameworks. *Science* **2013**, *341*, 1230444.
(32) Hoskins, B. F.; Robson, R. Design and Construction of a New Class of Scaffolding-Like Materials Comprising Infinite Polymeric Frameworks of 3D-Linked Molecular Rods. A Reappraisal of the Zinc Cyanide and Cadmium Cyanide Structures and the Synthesis and Structure of the Diamond-Related Frameworks $[N(Ch_3)_4][CuIZnII(CN)4]$ and CuI[4,4′,4″,4‴-Tetracyanotetraphenylmethane]-$BF_4.XC_6H_5NO_2$. *J. Am. Chem. Soc.* **1990**, *112*, 1546−1554.
(33) Kitagawa, S.; Kitaura, R.; Noro, S. Functional Porous Coordination Polymers. *Angew. Chem., Int. Ed.* **2004**, *43*, 2334−2375.
(34) Guillerm, V.; Kim, D.; Eubank, J. F.; Luebke, R.; Liu, X.; Adil, K.; Lah, M. S.; Eddaoud, M. A Supermolecular Building Approach for the Design and Construction of Metal−Organic Frameworks. *Chem. Soc. Rev.* **2014**, *43*, 6141−6172.
(35) Farha, O. K.; Hupp, J. T. Rational Design, Synthesis, Purification, and Activation of Metal−Organic Framework Materials. *Acc. Chem. Res.* **2010**, *43*, 1166−1175.
(36) Farha, O. K.; Eryazici, I.; Jeong, N. C.; Hauser, B. G.; Wilmer, C. E.; Sarjeant, A. A.; Snurr, R. Q.; Nguyen, S. T.; Yazaydin, A. O.; Hupp, J. T. Metal-Organic Framework Materials with Ultrahigh Surface Areas: Is the Sky the Limit? *J. Am. Chem. Soc.* **2012**, *134*, 15016−15021.
(37) Furukawa, H.; Ko, N.; Go, Y. B.; Aratani, N.; Choi, S. B.; Choi, E.; Yazaydin, A. Ö.; Snurr, R. Q.; O'Keeffe, M.; Kim, J.; Yaghi, O. M. Ultrahigh Porosity in Metal-Organic Frameworks. *Science* **2010**, *329*, 424−428.
(38) Wang, T. C.; Vermeulen, N. A.; Kim, I. S.; Martinson, A. B.; Stoddart, J. F.; Hupp, J. T.; Farha, O. K. Scalable Synthesis and Post-Modification of a Mesoporous Metal-Organic Framework Called NU-1000. *Nat. Protoc.* **2016**, *11*, 149−162.
(39) Wang, T. C.; Bury, W.; Gómez-Gualdrón, D. A.; Vermeulen, N. A.; Mondloch, J. E.; Deria, P.; Zhang, K.; Moghadam, P. Z.; Sarjeant, A. A.; Q.Snurr, R.; Stoddart, J. F.; T.Hupp, J.; Farha, O. K. Ultrahigh Surface Area Zirconium Mofs and Insights into the Applicability of the BET Theory. *J. Am. Chem. Soc.* **2015**, *137*, 3585−3591.
(40) Falkowski, J. M.; Liu, S.; Lin, W. Asymmetric Catalysis with Chiral Metal Organic Frameworks. *In Metal Organic Frameworks as Heterogeneous Catalysts*; The Royal Society of Chemistry: 2013; Chapter 11, pp 344−364.
(41) Lee, J.; Farha, O. K.; Roberts, J.; Scheidt, K. A.; Nguyen, S. T.; Hupp, J. T. Metal-Organic Framework Materials as Catalysts. *Chem. Soc. Rev.* **2009**, *38*, 1450−1459.
(42) Li, J. R.; Sculley, J.; Zhou, H. C. Metal-Organic Frameworks for Separations. *Chem. Rev.* **2012**, *112*, 869−932.
(43) Sumida, K.; Rogow, D. L.; Mason, J. A.; McDonald, T. M.; Bloch, E. D.; Herm, Z. R.; Bae, T.-H.; Long, J. R. Carbon Dioxide Capture in Metal−Organic Frameworks. *Chem. Rev.* **2012**, *112*, 724−781.
(44) Nugent, P.; Belmabkhout, Y.; Burd, S. D.; Cairns, A. J.; Luebke, R.; Forrest, K.; Pham, T.; Ma, S.; Space, B.; Wojtas, L.; Eddaoudi, M.; Zaworotko, M. J. Porous Materials with Optimal Adsorption Thermodynamics and Kinetics for CO2 Separation. *Nature* **2013**, *495*, 80−84.
(45) Cadiau, A.; Adil, K.; Bhatt, P. M.; Belmabkhout, Y.; Eddaoudi, M. A Metal-Organic Framework−Based Splitter for Separating Propylene from Propane. *Science* **2016**, *353*, 137−140.
(46) Kreno, L. E.; Leong, K.; Farha, O. K.; Allendorf, M.; Duyne, R. P. V.; Hupp, J. T. Metal-Organic Framework Materials as Chemical Sensors. *Chem. Rev.* **2012**, *112*, 1105−1125.
(47) Li, Q.-Y.; Ma, Z.; Zhang, W.-Q.; Jia-LongXu; Wei, W.; Lu, H.; Zhao, X.; Wang, X.-J. Aie-Active Tetraphenylethene Functionalized Metal-Organic Framework for Selective Detection of Nitroaromatic Explosives and Organic Photocatalysis. *Chem. Commun.* **2016**, *52*, 11284−11287.
(48) Klet, R. C.; Tussupbayev, S.; Borycz, J.; Gallagher, J. R.; Stalzer, M. M.; Miller, J. T.; Gagliardi, L.; Hupp, J. T.; Marks, T. J.; Cramer, C. J.; Delferro, M.; Farha, O. K. Single-Site Organozirconium Catalyst Embedded in a Metal−Organic Framework. *J. Am. Chem. Soc.* **2015**, *137*, 15680−15683.
(49) Ma, L.; Abney, C.; Lin, W. Enantioselective Catalysis with Homochiral Metal-Organic Frameworks. *Chem. Soc. Rev.* **2009**, *38*, 1248−1256.
(50) Zhang, W.-Q.; Li, Q.-Y.; Zhang, Q.; Lu, Y.; Lu, H.; Wang, W.; Zhao, X.; Wang, X.-J. Robust Metal−Organic Framework Containing Benzoselenadiazole for Highly Efficient Aerobic Cross-Dehydrogenative Coupling Reactions under Visible Light. *Inorg. Chem.* **2016**, *55*, 1005−1007.
(51) Miner, E. M.; Fukushima, T.; Sheberla, D.; Sun, L.; Surendranath, Y.; Dincă, M. Electrochemical Oxygen Reduction Catalysed by Ni_3(Hexaiminotriphenylene)$_2$. *Nat. Commun.* **2016**, *7*, 10942.
(52) Yuan, S.; Zou, L.; Li, H.; Chen, Y.-P.; Qin, J.; Zhang, Q.; Lu, W.; Hall, M. B.; Zhou, H.-C. Flexible Zirconium Metal-Organic Frameworks as Bioinspired Switchable Catalysts. *Angew. Chem., Int. Ed.* **2016**, *55*, 10776−10780.
(53) Islamoglu, T.; Atilgan, A.; Moon, S.-Y.; Peterson, G. W.; DeCoste, J. B.; Hall, M.; Hupp, J. T.; Farha, O. K. Cerium(IV) vs Zirconium(IV) Based Metal−Organic Frameworks for Detoxification of a Nerve Agent. *Chem. Mater.* **2017**, *29*, 2672−2675.
(54) Yang, D.; Odoh, S. O.; Wang, T. C.; Farha, O. K.; Hupp, J. T.; Cramer, C. J.; Gagliardi, L.; Gates, B. C. Metal−Organic Framework Nodes as Nearly Ideal Supports for Molecular Catalysts: NU-1000- and UiO-66-Supported Iridium Complexes. *J. Am. Chem. Soc.* **2015**, *137*, 7391−7396.
(55) Li, Z.; Peters, A. W.; Bernales, V.; Ortuño, M. A.; Schweitzer, N. M.; DeStefano, M. R.; Gallington, L. C.; Platero-Prats, A. E.; Chapman, K. W.; Cramer, C. J.; Gagliardi, L.; Hupp, J. T.; Farha, O. K. Metal−Organic Framework Supported Cobalt Catalysts for the Oxidative Dehydrogenation of Propane at Low Temperature. *ACS Cent. Sci.* **2017**, *3*, 31−38.
(56) Manna, K.; Ji, P.; Greene, F. X.; Lin, W. Metal−Organic Framework Nodes Support Single-Site Magnesium−Alkyl Catalysts for Hydroboration and Hydroamination Reactions. *J. Am. Chem. Soc.* **2016**, *138*, 7488−7491.

DOI: 10.1021/acsami.7b05494
ACS Appl. Mater. Interfaces 2017, 9, 24555−24560

(57) Liu, Y.; Howarth, A. J.; Hupp, J. T.; Farha, O. K. Selective Photooxidation of a Mustard-Gas Simulant Catalyzed by a Porphyrinic Metal-Organic Framework. *Angew. Chem., Int. Ed.* **2015**, *54*, 9001−9005.
(58) Liu, Y.; Buru, C. T.; Howarth, A. J.; Mahle, J. J.; Buchanan, J. H.; DeCoste, J. B.; Hupp, J. T.; Farha, O. K. Efficient and Selective Oxidation of Sulfur Mustard Using Singlet Oxygen Generated by a Pyrene-Based Metal−Organic Framework. *J. Mater. Chem. A* **2016**, *4*, 13809−13813.
(59) Deria, P.; Mondloch, J. E.; Tylianakis, E.; Ghosh, P.; Bury, W.; Snurr, R. Q.; Hupp, J. T.; Farha, O. K. Perfluoroalkane Functionalization of NU-1000 via Solvent-Assisted Ligand Incorporation: Synthesis and CO_2 Adsorption Studies. *J. Am. Chem. Soc.* **2013**, *135*, 16801−16804.
(60) Islamoglu, T.; Goswami, S.; Li, Z.; Howarth, A. J.; Farha, O. K.; Hupp, J. T. Postsynthetic Tuning of Metal−Organic Frameworks for Targeted Applications. *Acc. Chem. Res.* **2017**, *50*, 805−813.
(61) Hod, I.; Bury, W.; Gardner, D. M.; Deria, P.; Roznyatovskiy, V.; Wasielewski, M. R.; Farha, O. K.; Hupp, J. T. Bias-Switchable Permselectivity and Redox Catalytic Activity of a Ferrocene-Functionalized, Thin-Film Metal−Organic Framework Compound. *J. Phys. Chem. Lett.* **2015**, *6*, 586−591.
(62) Rimoldi, M.; Nakamura, A.; Vermeulen, N. A.; Henkelis, J. J.; Blackburn, A. K.; Hupp, J. T.; Stoddart, J. F.; Farha, O. K. A Metal-Organic Framework Immobilised Iridium Pincer Complex. *Chem. Sci.* **2016**, *7*, 4980−4984.
(63) Deria, P.; Li, S.; Zhang, H.; Snurr, R. Q.; Hupp, J. T.; Farha, O. K. A MOF Platform for Incorporation of Complementary Organic Motifs for CO_2 Binding. *Chem. Commun.* **2015**, *51*, 12478−12481.
(64) Deria, P.; Bury, W.; Hod, I.; Kung, C.-W.; Karagiaridi, O.; Hupp, J. T.; Farha, O. K. MOF Functionalization via Solvent-Assisted Ligand Incorporation: Phosphonates vs Carboxylates. *Inorg. Chem.* **2015**, *54*, 2185−2192.
(65) Deria, P.; Bury, W.; Hupp, J. T.; Farha, O. K. Versatile Functionalization of the NU-1000 Platform by Solvent-Assisted Ligand Incorporation. *Chem. Commun.* **2014**, *50*, 1965−1968.
(66) DeCoste, J. B.; Demasky, T. J.; Katz, M. J.; Farha, O. K.; Hupp, J. T. A Uio-66 Analogue with Uncoordinated Carboxylic Acids for the Broad-Spectrum Removal of Toxic Chemicals. *New J. Chem.* **2015**, *39*, 2396−2399.
(67) Deria, P.; Chung, Y. G.; Snurr, R. Q.; Hupp, J. T.; Farha, O. K. Water Stabilization of Zr6-Based Metal−Organic Frameworks via Solvent-Assisted Ligand Incorporation. *Chem. Sci.* **2015**, *6*, 5172−5176.
(68) Madrahimov, S. T.; Gallagher, J. R.; Zhang, G.; Meinhart, Z.; Garibay, S. J.; Delferro, M.; Miller, J. T.; Farha, Omar K.; Hupp, J. T.; Nguyen, S. T. Gas-Phase Dimerization of Ethylene under Mild Conditions Catalyzed by MOF Materials Containing (Bpy)NiII Complexes. *ACS Catal.* **2015**, *5*, 6713−6718.
(69) Howarth, A. J.; Buru, C. T.; Liu, Y.; Ploskonka, A. M.; Hartlieb, K. J.; McEntee, M.; Mahle, J.; Buchanan, J.; Durke, E.; Al-Juaid, S. S.; Stoddart, J. F.; DeCoste, J. B.; Hupp, J. T.; Farha, O. K. Postsynthetic Incorporation of a Singlet Oxygen Photosensitizer in a Metal-Organic Framework for Fast and Selective Oxidative Detoxification of Sulfur Mustard. *Chem. - Eur. J.* **2017**, *23*, 214−218.
(70) Zhan, X.; Facchetti, A.; Barlow, S.; Marks, T. J.; Ratner, M. A.; Wasielewski, M. R.; Marder, S. R. Rylene and Related Diimides for Organic Electronics. *Adv. Mater.* **2011**, *23*, 268−284.
(71) Ruoff, R. S.; Tse, D. S.; Malhotra, R.; Lorents, D. C. Solubility of Fullerene (C60) in a Variety of Solvents. *J. Phys. Chem.* **1993**, *97*, 3379−3383.
(72) Sauvé, G.; Fernando, R. Beyond Fullerenes: Designing Alternative Molecular Electron Acceptors for Solution-Processable Bulk Heterojunction Organic Photovoltaics. *J. Phys. Chem. Lett.* **2015**, *6*, 3770−3780.

DOI: 10.1021/acsami.7b05494
ACS Appl. Mater. Interfaces 2017, 9, 24555−24560